Localization of Hydrophobic Ions in Phospholipid Bilayers Using ^1H Nuclear Overhauser Effect Spectroscopy†

Jeffrey F. Ellena, Raymond N. Dominey,‡ Sharon J. Archer, Zhen-Chen Xu, and David S. Cafiso*
Department of Chemistry and Biophysics Program, University of Virginia, Charlottesville, Virginia 22901
Received November 26, 1986; Revised Manuscript Received February 27, 1987

ABSTRACT: The binding location for the hydrophobic ions tetraphenylphosphonium (TPP^+) and tetraphenylboron (TPB^-) was studied in sonicated phosphatidylcholine (PC) vesicles by measuring time-dependent and steady-state intermolecular ^1H nuclear Overhauser effects (NOE's). Intermolecular cross-relaxation was also investigated by two-dimensional NOE spectroscopy. Information on the distance and order parameter dependence of the NOE's was obtained from a simple simulation of the NOE's in the alkyl chain region. Taken together, the NOE data and the simulation provide strong evidence that TPB^- and TPP^+, at low concentrations ($\leq$10 mol %), are localized in the alkyl chain region of the bilayer. At these lower concentrations of TPP^+ or TPB^-, no significant effect on lipid ^{13}C T_1 or T_2 relaxation rates is detected. The proposed location is consistent with the expected free energy profiles for hydrophobic ions and with the carbonyl oxygens or interfacial water as the source of the membrane dipole potential. At higher ion/lipid ratios ($\geq$20 mol %), TPB^-/lipid NOE's increase. This results from a specific association of TPB^- with the choline head group.

Electrostatic energies are crucial in controlling ion transport rates across lipid bilayers. These energies play fundamental roles in a wide range of membrane-associated processes and are vital in determining the folding and conformational states of membrane proteins. For these reasons, the electrostatic structure of membranes has been of considerable interest. Hydrophobic ions are unique and powerful probes of the electrostatic structure of biological and model membrane systems. They exhibit several important and characteristic properties; for example, they are relatively membrane permeable and bind to interfacial regions of bilayers (Ketterer et al., 1971). The region in the membrane interface where these ions are localized is termed the "boundary" region (Andersen et al., 1978; McLaughlin, 1977). From a measure of the equilibrium-phase partitioning of these ions, the magnitude of the potential in the boundary region can be estimated (Cafiso & Hubbell, 1981). Measurements of transmembrane currents for these ions also provide information on the magnitude of the free energy barrier to transport [see, for example, Läuger et al. (1981) and Cafiso and Hubbell (1982)].

While hydrophobic ions share some common properties, hydrophobic anions and cations have dramatically different behaviors in phosphatidylcholine (PC) membranes. For structurally similar molecules, such as TPB^- and TPP^+,[1] it is found that TPB^- has a rate constant for membrane transport that is several orders of magnitude larger than that for TPP^+ (Pickar & Benz, 1978; Cafiso & Hubbell, 1982). TPB^- also binds much more strongly than TPP^+ to the membrane interface (Flewelling & Hubbell, 1986a). This large difference in binding and translocation rates is apparently due to the interaction of these ions with the membrane dipole field. Recently, a model was presented that accounted for the differences in both binding and translocation rates by incorporating the membrane dipole potential into a total energy profile for these ions in the membrane (Flewelling & Hubbell, 1986b). The expected energy profiles for hydrophobic cations and anions, calculated by using this model, are shown in Figure 1. Several important predictions regarding the properties of these ions are illustrated in this figure. For example, both TPP^+ and TPB^- are expected to be localized within the membrane–solution interface, and TPB^- is expected to bind slightly deeper in the interface than TPP^+. This model also predicts that the boundary region (where hydrophobic ions bind) should lie a few angstroms deeper than the molecular dipole layer giving rise to the dipole potential.

Direct information on the location of these ions within the membrane interface would be extremely useful. This information could provide direct evidence for the interaction of these ions with the membrane dipole layer and would aid in defining the molecular source of the dipole field. Localizing these ions would also permit boundary potentials and dielectric constants to be assigned to a specific region within the membrane interface.

The interactions of hydrophobic ions with membranes were previously investigated by NMR spectroscopy. Phenyl ring current shifts induced in ^1H lipid resonances were used to localize $TPMP^+$ (tetraphenylmethylphosphonium) and TPB^- in PC bilayers (Levine et al., 1979). In addition, ^2H, ^{13}C, and ^{14}N NMR techniques were employed under similar conditions to determine both the location and conformational changes induced by the binding of these ions (Hubbell et al., 1980; Siminovitch et al., 1984). These experiments indicate that the predominant interactions of hydrophobic ions occur with the lipid head group. While this information reveals important properties regarding the interaction of hydrophobic ions with

† This work was supported by a grant from the National Institutes of Health (GM35215) and the Dreyfus Foundation Award for New Faculty in Chemistry (both to D.S.C.).
* Correspondence should be addressed to this author at the Department of Chemistry.
‡ Present address: Department of Chemistry, University of Richmond, Richmond, VA 23173.

[1] Abbreviations: NMR, nuclear magnetic resonance; NOE, nuclear Overhauser effect; TPB^-, tetraphenylboron; TPP^+, tetraphenylphosphonium; $TPMP^+$, triphenylmethylphosphonium; $TPHP^+$, triphenylhexadecylphosphonium; N-Me, *N*-methyl; T_1, spin–lattice relaxation time; T_2, spin–spin relaxation time; egg PC, egg phosphatidylcholine; POPC, palmitoyloleoyl-PC.

0006-2960/87/0426-4584$01.50/0

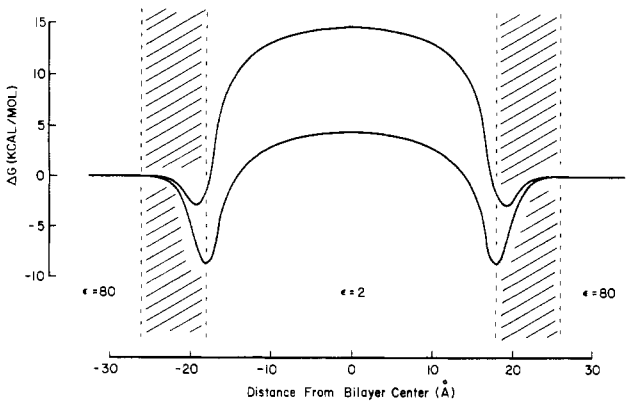

FIGURE 1: Free energy diagram for TPP^+ (upper curve) and TPB^- (lower curve) modeled by using both binding and kinetic data for hydrophobic ions [this model was devised by Flewelling and Hubbell (1986)]. The curves shown here were calculated by using the optimized parameters given previously. The dipole layer giving rise to the membrane dipole potential is at a distance of 22 Å from the bilayer center and the membrane dielectric constant undergoes a transition from $\epsilon = 2$ to $\epsilon = 80$ in the shaded region of the diagram. The differences in the curves for the hydrophobic cation and anion are a result of the membrane dipole potential.

membranes, the experiments were carried out at extremely high concentrations of ions. The binding energies for these ions begin to change significantly above ca. 1 mol % [presumably due to electrostatic charging of the boundary region; see Neumcke and Läuger (1970), LeBlanc (1969), Andersen et al. (1978), and Flewelling and Hubbell (1986)]. Therefore, previous measurements do not necessarily reflect the binding that is expected under typical probe concentrations. At these high ion concentrations, the free energy profiles shown in Figure 1 will be altered by an additional electrostatic interaction.

In this paper, we describe the measurement of ^1H nuclear Overhauser effects that occur between hydrophobic ions and membrane lipids. We measure NOE's for the hydrophobic ions tetraphenylboron and tetraphenylphosphonium at both high and low ion concentrations. The results are used to determine the region where these ions are located in bilayers. We also model the cross-relaxation behavior measured here using a simple model for the buildup of steady-state 1D NOE's. The results of this study provide direct evidence that these ions, at typical probe concentrations, are located within the membrane hydrocarbon region.

Experimental Procedures

Materials. Egg phosphatidylcholine was purified from fresh hen eggs according to the procedure of Singleton et al. (1965) and stored in chloroform under an argon atmosphere at −20 °C. Deuterium oxide, sodium tetraphenylboron, and tetraphenylphosphonium chloride were obtained from Aldrich Chemical Co. (Milwaukee, WI).

Preparation of Phospholipid Vesicles. To prepare unilamellar phospholipid vesicles, aliquots of egg PC were dried under vacuum for at least 15 h, dispersed in a D_2O buffer containing 100 mM phosphate buffer, pD 7.0, and ultrasonically irradiated for approximately 40 min. The sonicated lipid suspensions were then centrifuged at ca. 30000*g* for 20 min to remove titanium dust from the sonicator tip and float any unsonicated lipid. Unless otherwise specified, hydrophobic ions were added to the lipid chloroform solution and dried with the lipid. No noticeable decomposition of either TPB^- or TPP^+ was observed following sonication, as judged by ^1H NMR. At the concentrations of hydrophobic ion used here, no major changes in the morphology of the vesicle suspensions were seen (as determined by light scattering and electron microscopy). At concentrations of TBP^- higher than those used here, dramatic changes in the morphology of egg PC vesicles containing TPB^- can be observed (Cafiso and Hubbell, unpublished).

Measurement of the Partitioning of Hydrophobic Ions. Concentrations of TPP^+ or TPB^- in aqueous solution were determined spectrophotometrically. We measured the phase partitioning for the hydrophobic ion by measuring its concentration in the initial filtrate from a Centricon microconcentrator (Amicon, Danvers, MA). The partition coefficient for TPP^+ was determined as previously described (Flewelling & Hubbell, 1986) by using eq 1, where C_f^0 and C_f are the

$$C_f^0/C_f = 1 + A_L C_L(\beta - V_L/A_L) \quad (1)$$

concentrations of aqueous ion in the absence and presence of vesicles, respectively, A_L and V_L are the areas and volumes per phospholipid, and C_L is the phospholipid concentration.

NMR Spectroscopy. NMR spectra were obtained by using a Nicolet NT-360 spectrometer operating at a proton frequency of 361.065 MHz and a carbon-13 frequency of 90.793 MHz (magnetic field strength 8.47 T). The sample temperature during all experiments was 25 ± 1 °C. All 180° pulses were 90*x*, 180*y*, 90*x* composite pulses. The fast inversion recovery method (Craik & Levy, 1984) was used to obtain ^{13}C spin–lattice relaxation times (T_1). Modulated ^1H decoupling was used throughout the T_1 experiments. The Carr Purcell Meiboom Gill experiment was used to obtain ^{13}C spin–spin relaxation times (T_2). Modulated ^1H decoupling was used at all times except during the ^{13}C pulses and the echo period. The delay between refocusing pulses was typically 2 ms. No dependence of T_2 was found on the delay between refocusing pulses when the delay was varied from 2 to 8 ms. The recycle delay for T_2 experiments was at least 5 times T_1 for all resonances except the fatty acyl methyl resonance (≈3 times T_1).

In one-dimensional NOE experiments, the acquisition of control spectra and spectra with individual resonances saturated was alternated. For all 1D NOE experiments, a saturating field strength between 23 and 27 Hz was used, and the recycle delay was at least 5 times the longest T_1. The buildup rate of the steady-state NOE was monitored by performing truncated NOE experiments as described by Wagner and Wüthrich (1981).

Two-dimensional cross-relaxation (2D NOE) spectra were obtained in absolute value mode as previously described (Ellena et al., 1985). Phase-sensitive 2D NOE spectra were obtained with the same pulse sequence, along with the appropriate pulse phase cycling and data collection routines (States et al., 1982). Gaussian multiplication (20 Hz) was applied to both dimensions of the phase-sensitive 2D NOE spectra. Spectra were zero-filled once in the first dimension, yielding a final data size of 256 × 256 points for the absorptive part of the spectrum.

Simulation of Proton Cross-Relaxation in Membranes. The time-dependent and steady-state NOE's were simulated by using a simple model spin system. Here, the time-dependent nuclear Overhauser effect is defined as

$$\eta_i(t) = (I_{zi}(t) - I_{0i})/I_{0i} \quad (2)$$

where $I_{zi}(t)$ is the intensity of spin i after saturation at time t and I_{0i} is the intensity of spin i at equilibrium. For a system of dipolar coupled spins, the values of I_{zi} are described by a series of coupled differential equations (Noggle & Schirmer, 1971):

$$dI_{zi}/dt = -\rho_i(I_{zi} - I_{0i}) - \sum_{j \neq i} \sigma_{ij}(I_{zj} - I_{0j}) \quad (3)$$

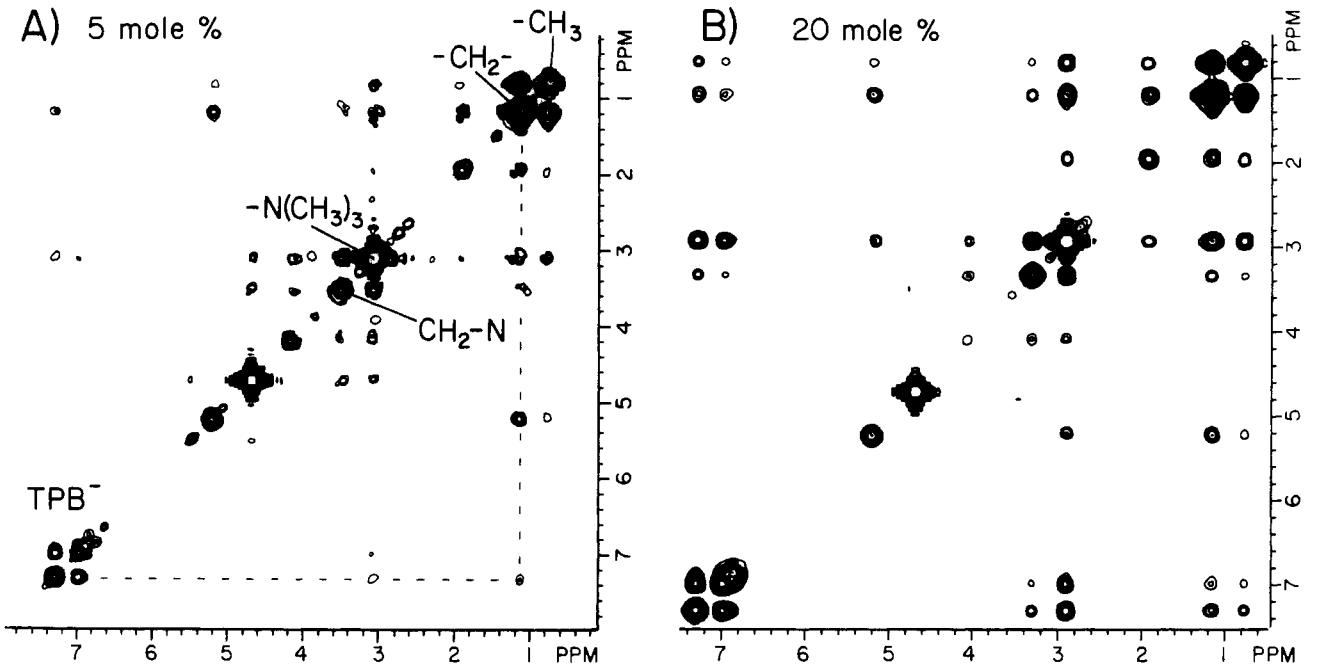

FIGURE 2: Two-dimensional NOE spectra in absolute value mode for sonicated egg PC vesicles (130 mM egg PC in 100 mM NaPhos, pD 7) containing (A) 5 mol % TPB^- and (B) 20 mol % TPB^-. The assignments of the TPB^- phenyl resonances are ortho, meta, para (low field to high field). The mixing time for each spectrum was 300 ms, and the data consisted of 128 blocks with 256 data points per block. Each block was the result of 32 acquisitions.

Here, ρ_i is the direct relaxation rate of spin i due to all other spins and σ_{ij} is the cross-relaxation rate between spins i and j. In our simulation, we assumed an instantaneous saturation of one or more spins in the system and used a solution given previously to determine the values of $\eta_i(t)$ [see Dobson et al. (1982)]. In matrix form this solution is

$$[\eta] = [\Gamma]^{-1}[\sigma] - [T]\exp(-[D]t)[T]^{-1}[\Gamma]^{-1}[\sigma] \quad (4)$$

Here, $[D] = [T]^{-1}[\Gamma][T]$, [D] is the diagonal matrix containing the eigenvalues of the relaxation matrix $[\Gamma]$, and [T] is the matrix composed of the eigenvectors of $[\Gamma]$. $[\Gamma]$ is a square matrix of dimension $n - j$, where n is the number of spins in the system and j is the number of saturated spins. $[\sigma]$ is the cross-relaxation matrix containing terms for the interaction between saturated and observed spins [for further details see Dobson et al. (1982)]. The direct and cross-relaxation rates, ρ_i and σ_{ij}, respectively, were estimated by using

$$\rho_i = \frac{\hbar^2\gamma^4}{10}\sum_{j\neq i}\frac{1}{r_{ij}^6}[3J(2\omega) + 1.5J(\omega) + 0.5J(0)] \quad (5)$$

$$\sigma_{ij} = \frac{\hbar^2\gamma^4}{10}\frac{1}{r_{ij}^6}[3J(2\omega) - 0.5J(0)] \quad (6)$$

Here, r_{ij} is the distance between spins i and j, γ is the magnetogyric ratio for protons, and $J(2\omega)$, $J(\omega)$, and $J(0)$ are the spectral densities corresponding to double, single, and zero quantum transitions, respectively (Noggle & Schirmer, 1971). Because of the qualitative nature of the conclusions we derive from this simulation, we used a simple spectral density function for the motion of spins in a small bilayer vesicle. We assume that the spin system undergoes a slow isotropic motion with a correlation time of 1 μs, τ_c^s [due to vesicle tumbling and lateral diffusion; see Burnell et al. (1980) and references cited therein)]. We also assume that there is a much shorter correlation time, τ_c^f (in the range of 10–100 ps) that represents bond isomerizations and torsions in the alkyl chains (Pace & Chan, 1982; Brown, 1982). The fast motion is of limited amplitude and is characterized by an order parameter for dipolar interactions, S_{HH}. In this case

$$J(\omega) = (1 - S_{HH}^2)J^f(\omega) + S_{HH}^2J^s(\omega) \quad (7)$$

where $J^{f,s}(\omega) = 2\tau_c^{f,s}/(1 + (\omega\tau_c^{f,s})^2)$. To simulate the hydrophobic ion alkyl chain NOE's, we calculated ρ_i and σ_{ij} with the assumption that the ion undergoes an isotropic motion with a correlation time of 1×10^{-8} s.[2]

RESULTS

Tetraphenylborate/Lipid Cross-Relaxation Is Concentration Dependent. Shown in Figure 2 are two-dimensional ^1H NMR spectra in absolute value mode for TPB^- bound to egg PC vesicles. At the concentration of lipid used here, this hydrophobic anion is completely membrane associated.[3] In Figure 2B, a spectrum at 300-ms mixing time is shown for a "high" concentration of TPB^-, 20 mol %. The predominant cross-relaxation in this case occurs between the ortho position on the phenyl resonances of TPB^- and the N-Me head-group resonance. Cross-relaxation among the lipid-proton resonances is also dramatically enhanced relative to vesicles free of TPB^-. At lower concentrations of TPB^-, the pattern of cross-relaxation is clearly altered relative to that shown in Figure 2B. As shown in Figure 2A, where TPB^- is added to 5 mol %, the cross-peaks between TPB^- and the N-Me resonance are dramatically reduced (this corresponds to a 10-fold decrease in

[2] We estimated the correlation time for the diffusion of the hydrophobic ion using the expression $\tau_c = 4\pi R^3\eta/3kT$, where R is the radius of the hydrophobic ion (ca. 4.2 Å) and η is the value for the viscosity of the bilayer. We used a value of 1 P for the viscosity of the membrane (Pace & Chan, 1982). Similar correlation times have been found for fluorescent probes in bilayers (Mulders et al., 1986).

[3] The partition coefficient for TPB^- binding to lipid bilayers has been estimated to be ca. 3×10^{-2} cm (Andersen et al., 1978). Using this partition coefficient and eq 1, we estimated the phase partitioning of this negative hydrophobic ion. At the concentrations of egg PC vesicles used here, we find that less than 0.01% of this ion will be in the aqueous phase. Therefore, we treat TPB^- as a completely membrane-associated hydrophobic ion.

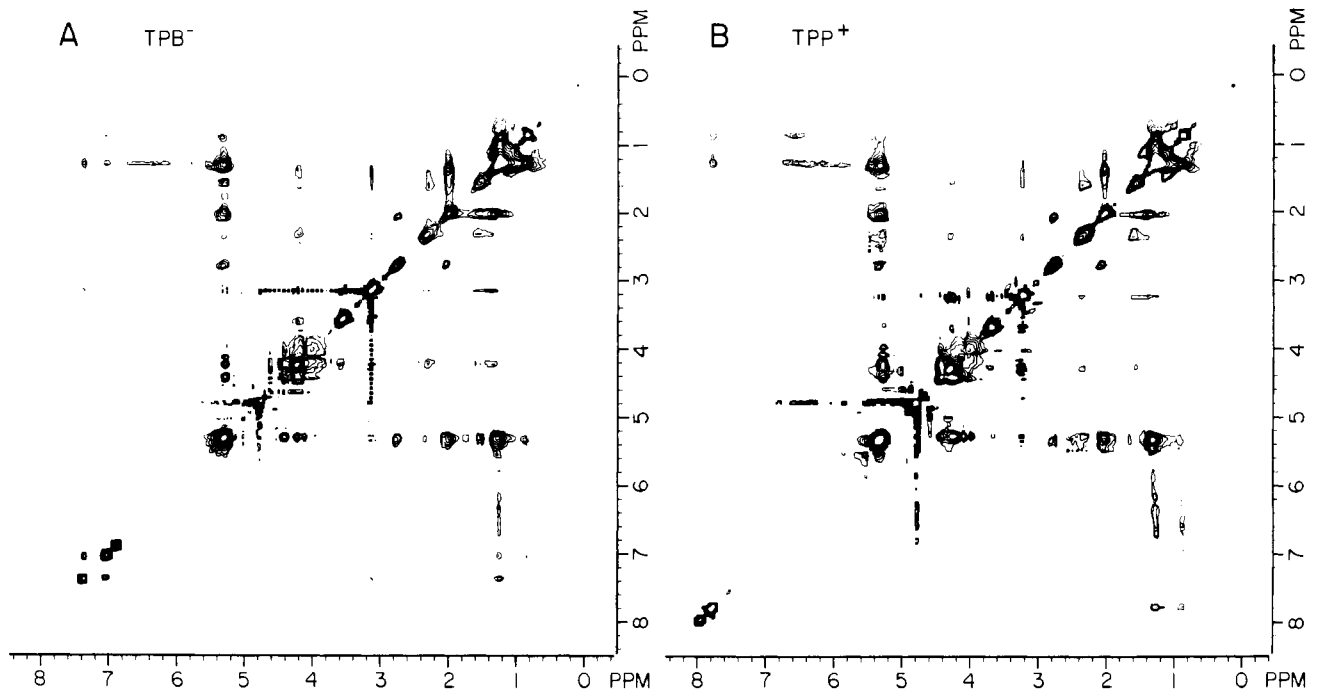

FIGURE 3: Pure absorption phase two-dimensional NOE spectra of (A) TPB^- and (B) TPP^+ incorporated into egg PC vesicles at a concentration of 10 mol %. The mixing time, τ_m, in these spectra was set to 100 ms. Gaussian multiplication (20 Hz) was applied to both dimensions of the spectra, and the spectra were zero-filled once in the first dimension to yield a final data size of 256 × 256 points for the absorptive part of the spectrum. At the concentration of lipid used here all TPB^- is bound, and the ratio of aqueous/membrane TPP^+ is ≈1.1.

the cross-relaxation rate between TPB^- and lipid). In addition, the largest cross-peaks are no longer seen with the N-Me resonance, but with the bulk methylene resonance $(CH_2)_n$. Cross-relaxation rates among the lipid protons are also reduced and are much closer to those seen in pure egg PC vesicles (Ellena et al., 1985).

We examined the pure absorption phase two-dimensional NOE spectra of TPP^+ and TPB^- at 10 mol % ion. Pure absorption phase 2D spectra generally have less overlap and distortion than absolute value spectra (States et al., 1982; Morris, 1986). As shown in Figure 3 the predominant cross-relaxation (at modest concentrations of hydrophobic ion) occurs between the hydrophobic ion phenyl ring (the ortho position for TPB^-, the ortho and meta positions for TPP^+) and the methylene resonance, $(CH_2)_n$.

Magnitudes of Steady-State Hydrophobic Ion/Membrane Lipid NOE's. Shown in Figure 4 are the steady-state NOE's measured for the largest TPB^- or TPP^+ resonances (the ortho and ortho–meta, respectively) when the indicated lipid resonances are selectively preirradiated for 7 s. NOE's obtained with 10 and 4 mol % hydrophobic ion are shown. Saturation of the methylene protons, $(CH_2)_n$, produces the largest NOE's. However, large NOE's are also observed when protons adjacent to the carbonyl or terminal methyl protons are saturated. Steady-state NOE's that result from saturation of the glycerol and head-group region are much smaller than those that develop from saturation of the alkyl chain region. While the NOE's for TPB^- and TPP^+ have similar dependencies on the lipid position saturated, the NOE's for TPB^- are uniformly larger than for TPP^+. We demonstrate below that this difference is simply due to phase-partitioning differences between these ions. As seen in Figure 4, the magnitude of the NOE's for 4 mol % TPB^- decreases slightly from the NOE's with 10 mol % ion, with the largest decrease occurring at the N-Me position. In contrast, the NOE's with 4 mol % TPP^+ are slightly larger than at the higher ion concentration.

The pattern of steady-state NOE's seen in Figure 4 indicates that the largest membrane/hydrophobic ion NOE's arise from

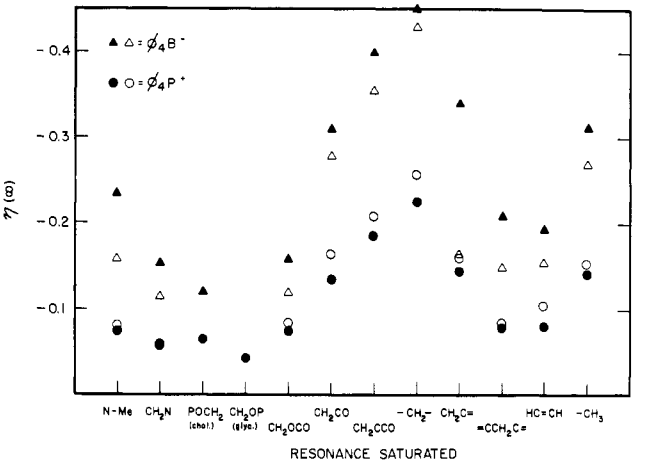

FIGURE 4: Steady-state NOE's measured for the ortho TPB^- and ortho–meta TPP^+ resonances after irradiating the indicated lipid resonances for 7 s. NOE's were measured for 10 mol % TPB^- (▲), 4 mol % TPB^- (△), 10 mol % TPP^+ (●), and 4 mol % TPP^+ (○). The errors in the values of η (7s) are ±1.2% for the cases where 10 mol % ion is present (▲, ●) and ±2 % for the cases where 4 mol % ion is present (△, ○). The CH_2OCO glycerol protons are inequivalent, and the higher field peak was saturated. Approximately 47% of the TPP^+ is membrane bound.

the alkyl chain region of the vesicle phospholipid. As shown below, a simulation of the cross-relaxation rates in this type of system indicates that the steady-state NOE is expected to be strongly dependent upon distance, even in the presence of significant spin diffusion. Thus, the data in Figure 4 provide strong evidence for the location of hydrophobic ions in the alkyl chain region of the bilayer.

When the phenyl resonances of TPP^+ or TPB^- are saturated, the NOE's detected in the lipid resonances are very small (a few percent) and are not shown here.

Time-Dependent, Truncated NOE's for TPP^+ and TPB^-. We examined the time dependence of several NOE's shown in Figure 4. The time-dependent NOE's for TPB^- or TPP^+, when several alkyl chain resonances are saturated, are shown

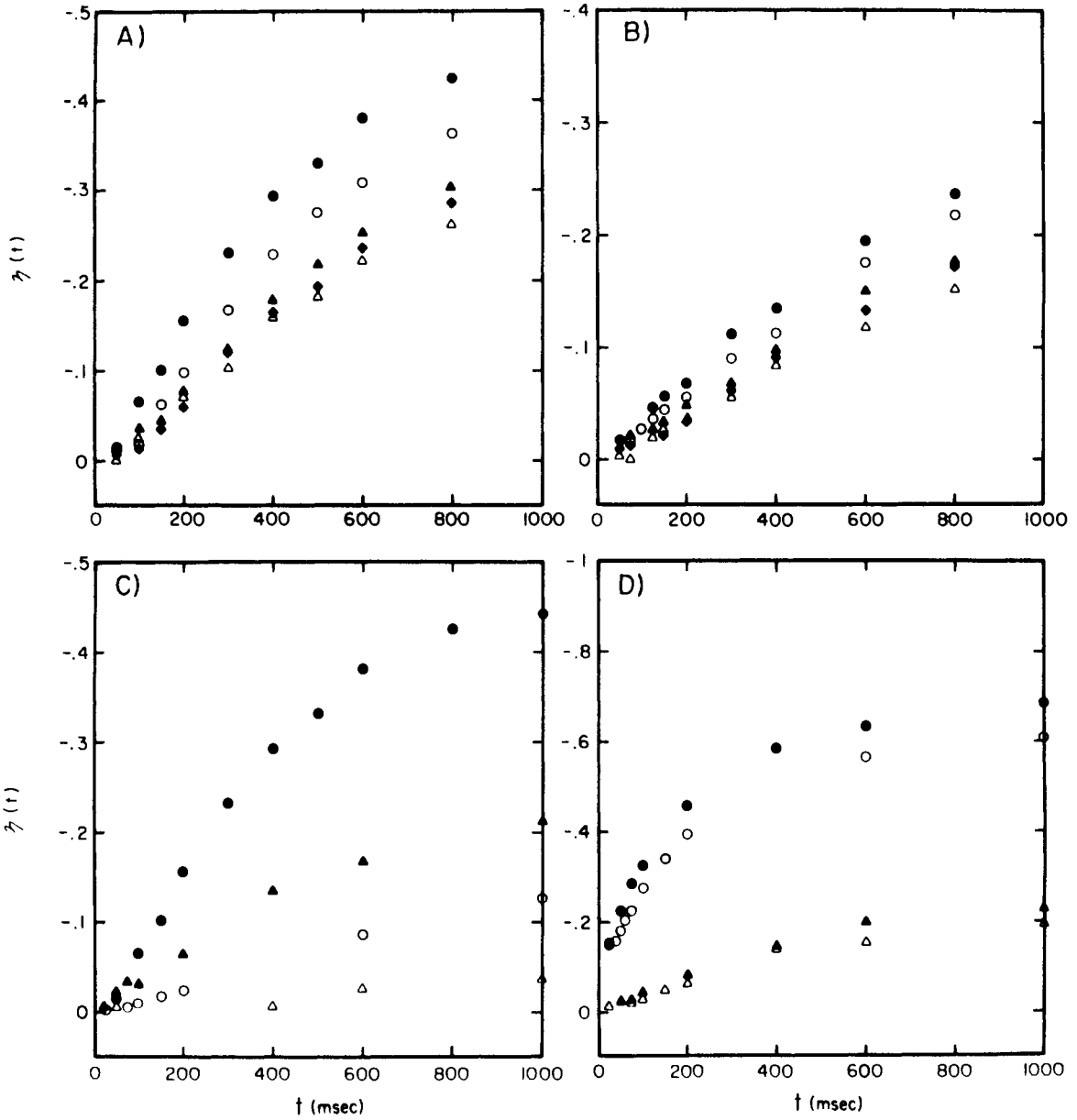

FIGURE 5: Time-dependent NOE's measured in egg PC vesicles containing 10 mol % TPB^- or TPP^+ (here 100% of the TPB^- and ≈47% of the TPP^+ are membrane bound). (A) Time dependence of the TPB^- NOE at the ortho resonance when the CH_2 (●), CH_2CH_2COO (○), $CH_2C{=}$ (▲), CH_3 (◆), and CH_2COO (△) resonances are saturated. (B) Time dependence of the TPP^+ ortho–meta resonance when the lipid resonances indicated in (A) are saturated. (C) Time-dependent NOE's for TPB^- when the CH_2 (●) or N-Me (▲) resonances are saturated and for TPP^+ when the CH_2 (○) or N-Me (△) resonance is saturated. (D) Time dependence for the NOE at the CH_3 protons when the CH_2 resonance is saturated in the presence of TPP^+ (○) or TPB^- (●) and the NOE at the CH_3 protons when the CH_2COO resonance is saturated in the presence of TPP^+ (△) or TPB^- (▲).

in parts A and B of Figure 5, respectively. The general trends in the data reflect the differences seen in the steady-state NOE's (Figure 4). For TPP^+ and TPB^-, the buildup rates have the following order: $(CH_2)_n > CH_2CH_2COO > CH_2C{=}C > CH_2COO \approx CH_2CH_3$. The rates observed for saturation of the single allyl resonance are slightly higher than those observed for saturation of either the first methylene position in the acyl chain or the terminal methyl position. The factors that are important in determining these rates and the interpretation of this data in terms of the hydrophobic ion location are discussed below. When buildup rates are compared for lipid resonances in other regions of the bilayer, large differences in the rates are seen. In Figure 5C, the NOE's for TPP^+ or TPB^- are compared when either the lipid N-Me or CH_2 resonances are saturated. The fastest buildup rates are seen for saturation of the alkyl chain resonances. Again these data provide evidence that hydrophobic cations and anions are localized in the alkyl chain region of the lipid bilayer.

Phase-Partitioning Differences Account for TPP^+/TPB^- NOE Differences. There are several possible sources for the large differences between the NOE magnitudes seen for TPB^- and TPP^+ resonances. A diminished dipolar order parameter, S_{HH} associated with the lipid/hydrophobic ion dipolar interaction) for TPP^+ compared with TPB^- could account for these differences. This is not unexpected, since evidence for enhanced molecular order parameters for membrane lipid in the presence of TPB^- was previously observed (Seidah et al., 1976). At the lower concentrations of hydrophobic ion used here, there do not appear to be major differences in lipid ordering. In Figure 5D, for example, only small differences in the time-development of the terminal methyl/chain NOE's can be detected when TPP^+ and TPB^- samples are compared. The presence of 10 mol % TPB^- or TPP^+ has no significant effect

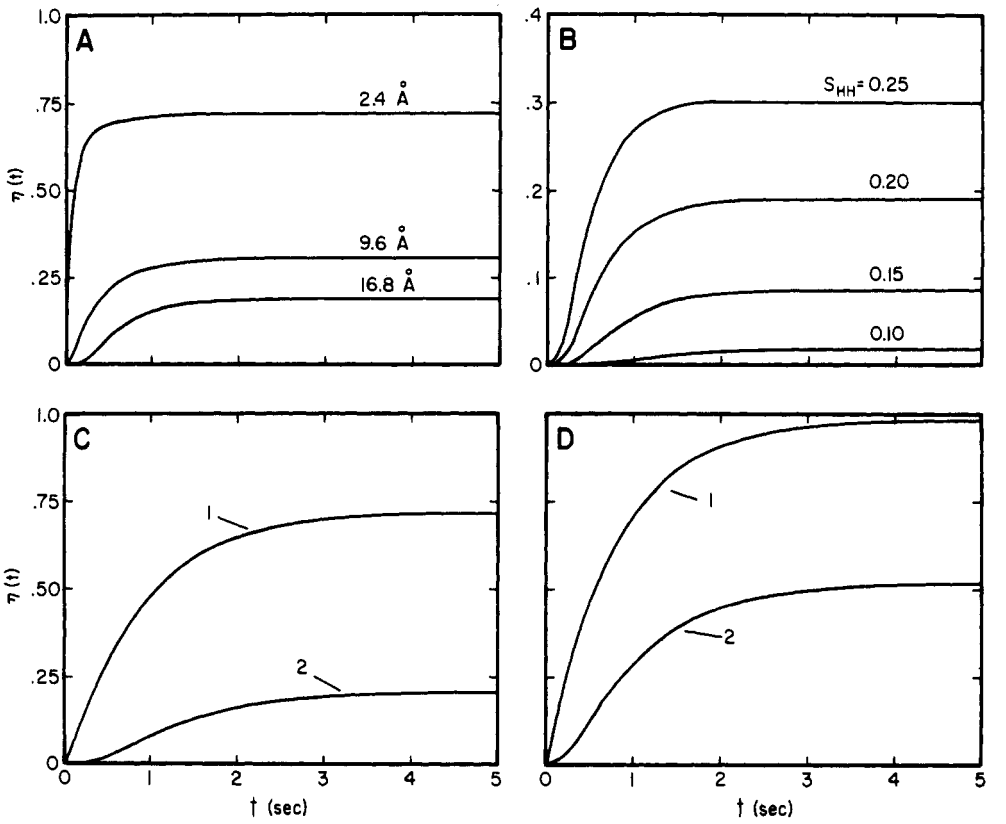

FIGURE 6: Time-dependent NOE's simulated for a simple model system using eq 4–7 described in the text. The model system consists of a linear chain of eight pairs of spins, where the distance between each member of a pair is 1.8 Å, and the distance between spins on adjacent pairs is 2.4 Å. The dipolar order parameter S_{HH} (eq 7) describes the interaction between spins on the chain. Except where noted, S_{HH} has a value of 0.2. In (C) and (D) an additional spin is included that moves independently of the chain with an isotropic correlation time of 1×10^{-8} s. Values for τ_c^f and τ_c^s are set to 1×10^{-6} and 5×10^{-11} s, respectively (see text). (A) One spin pair at the end of the chain is saturated at $t = 0$. NOE's observed for spin pairs at distances of 2.4, 9.6, and 16.8 Å are plotted. (B) One pair of spins at the end of the chain is saturated, and the observed NOE at the opposite end of the chain (16.8 Å away) is measured. The plot shows the dependence of the NOE for several different values of the dipolar order parameter, S_{HH}. (C) One spin pair at the end of the chain is saturated at $t = 0$. The NOE is observed for an additional detached spin at a distance of 3 Å from the chain. In (1), the observed spin is directly over the spin pair 2.4 Å from the saturated spin pair. In (2), the observed spin is directly over the pair 14.4 Å from the saturated spin at the end of the chain. (D) Four spin pairs at one end of the chain are saturated. The additional spin, as in (C), is detached and at a distance of 3 Å from the chain. The configurations 1 and 2 are as given in (C), above.

on the vesicle phospholipid ^{13}C T_1 and T_2 relaxation times (see below).

Another source for the NOE differences between hydrophobic cations and anions could be a difference in the phase partitioning of the two ions. At the concentrations of lipid used here, TPB^- will be entirely membrane associated. However, the negative free energy of binding is about 5 kcal/mol lower for TPP^+ than for TPB^- (presumably as a result of the membrane dipole potential), and a significant amount of TPP^+ is expected to be present in the aqueous phase. We measured the partitioning of TPP^+ in the lipid samples used here for ^1H NOE experiments. At 100 mg/mL lipid and 10 mol % TPP^+, the ratio of aqueous to membrane-associated TPP^+ is 1.1:1. We measure an effective partition coefficient for TPP^+ binding to egg PC of 2×10^{-6} under these conditions. This partition coefficient increases as the ratio of ion to lipid is decreased, due to a decrease in electrostatic interactions between TPP^+ ions in the interface. Under the conditions used here, the NOE is expected to increase proportionally with the increase in bound hydrophobic ion, in a manner analogous to the transferred NOE experiment described previously (Clore & Gronenborn, 1983).

The fraction of bound TPP^+ was changed by holding the lipid to TPP^+ ratio constant and varying the concentrations. The NOE's that were measured increased proportionally with the increase in bound TPP^+ and approached the steady-state NOE values for TPB^- when the population of aqueous TPP^+ was low (data not shown). NOE's were measured for triphenylhexadecylphosphonium ($TPHP^+$), a derivative of TPP^+. $TPHP^+$ has a much larger binding constant than TPP^+ because of its long alkyl chain and is totally membrane associated. The magnitudes of the NOE's seen for $TPHP^+$ resemble those seen for TPB^-. These data indicate that the NOE differences seen between the TPP^+ and TPB^- are simply a result of the phase-partitioning differences of these ions.

T_2 ^{13}C Relaxation Data for PC Vesicles Containing Hydrophobic Ions. Shown in Table I are T_2 relaxation rates for egg PC vesicles with and without 10 mol % TPP^+ or TPB^-. T_1 ^{13}C relaxation rates for egg PC without and with 10 mol % TPP^+ or TPB^- were also measured (data not shown). TPP^+ and TPB^- have either a very small or insignificant effect on the T_2 and T_1 values for all membrane lipid resonances measured. Thus, TPP^+ and TPB^-, when present at low concentrations (≤10 mol %), do not substantially alter membrane lipid conformation and dynamics.

Simulated Proton Cross-Relaxation Curves in a System of Dipolar-Coupled Spins. Figure 6 shows simulated NOE buildups for an eight-carbon methylene chain (Figure 6A,6B) and for the same chain adjacent to an unattached spin (Figure 6C,6D). These simulations are rough approximations of several experimental NOE's presented above and are intended to indicate, in a qualitative way, the importance of various factors in determining the observed NOE's. All parameters used in the simulations are listed in the figure legend. Figure

Table I: ^{13}C Spin–Spin Relaxation Rates in Sonicated Egg PC Vesicles

resonance	$1/T_2$ (s^{-1}) egg PC	PC + 10% TPB^-	PC + 10% TPP^+
$N(CH_3)_3^+$	5.6 ± 0.6	5.9 ± 1.0	5.9 ± 0.7
CH_2N	8.3 ± 1.5	9.2 ± 0.8	10.0 ± 1.0
CH_2COO	18.0 ± 2.0	23.0 ± 3.0	18.0 ± 4.0
CH_2CH_2COO	14.0 ± 1.0	16.0 ± 1.0	16.0 ± 3.0
$(CH_2)_n$	12.0 ± 1.0	14.0 ± 1.0	13.9 ± 1.0
HC=CH (1)	8.3 ± 1.3		10.0 ± 1.0
HC=CH (2)	11.0 ± 2.0		9.2 ± 0.8
$HC{=}CHCH_2HC{=}CH$	8.3 ± 1.4	11.0 ± 1.0	
$CH_2CH_2CH_3$	6.7 ± 0.8		9.1 ± 0.8
CH_2CH_3	5.5 ± 0.9	7.1 ± 0.5	6.3 ± 0.7
CH_3	4.3 ± 0.4	4.2 ± 0.2	3.8 ± 0.6

6A shows the dependence of the NOE on the distance between saturated and observed methylene groups. The NOE's (time-dependent and steady-state) depend heavily on the distance between observed and irradiated spins. Similar results are obtained when order parameters and correlation times are varied over the range commonly found in phospholipid membranes. It should be noted that under the conditions of these simulations, a substantial amount of spin diffusion takes place. Figure 6B shows the dependence of the NOE occurring between chain ends on order parameter. The NOE's become more negative as the order parameter increases because the spectral density due to slower motions increases (eq 7). Parts C and D of Figure 6 show the effect of saturating several chain positions on the NOE between the chain and a spin located adjacent to the chain. Even when several spins are saturated, the NOE's between the chain and the adjacent spin are highly dependent on the position of the adjacent spin.

Several factors were not taken into account in this simulation, which are important in membranes. These include intermolecular chain interactions; the inequivalence of geminal, vicinal, and longer range order parameters; and ordering of the hydrophobic ions. More realistic simulations would include these factors and are in progress. The curves shown in Figure 6 and other similar simulations indicate that both NOE buildup and steady-state experiments can provide information on the distance between observed and saturated spins, even though other factors (segmental ordering and spin diffusion) make important contributions to the observed NOE's.

Discussion

There are numerous techniques that could be utilized to provide information on the location of hydrophobic ions in membranes. We chose to use proton cross-relaxation because its high sensitivity permitted measurements to be made at relatively low concentrations of ions. The data shown above indicate that the intramembrane location of TPB^- is concentration dependent. The strong TPB^-/choline NOE's seen at concentrations greater than 20 mol % ion suggest that the ion complexes with the choline headgroup. This is consistent with observations (at high concentrations of TPB^-) of large phenyl ring current shifts in the head group (Levine et al., 1979), large changes in the ^{31}P NMR chemical shielding anisotropy (Siminovitch et al., 1984), and changes in the order parameters for head-group spin-labeled PC (Seidah et al., 1976). TPB^- has also been observed to induce fusion in small sonicated egg PC vesicles (Cafiso and Hubbell, unpublished results). In solution, TPB^- forms a precipitate with choline.

In our present study, we were primarily interested in characterizing the behavior of these ions at low concentrations, where their binding should reveal the position of the free energy minima shown in Figure 1. The NOE pattern at low concentrations of TPB^- is quite different than at higher concentrations and indicates that TPB^-/phospholipid cross-relaxation takes place primarily in the alkyl chain region of the bilayer. In the range of 4–10 mol % ion, only minor changes in the NOE pattern are seen. A similar NOE pattern for TPP^+ is observed for 10–4 mol % ion (bound concentrations of 5 mol % to less than 2 mol %). The decrease in the magnitude of the NOE's for TPP^+ with increasing concentration is likely the result of partitioning changes due to electrostatic effects.

Our simulations show that the steady-state NOE's are strongly influenced by segmental order, and this must be considered when interpreting the experimental results. It is well-known that segmental order is greatest in the glycerol region of the membrane phospholipid and decreases as one proceeds to either end of the molecule [see Seelig and Seelig (1980)]. The segment position dependence of phospholipid/hydrophobic ion steady-state NOE's does not parallel the position dependence of segmental order; therefore, segmental order does not dominate the steady-state NOE's. The simulations show that the steady-state NOE's are highly dependent on the distance between saturated and observed spins, and we conclude that the NOE's are determined primarily by distance and the number of spins saturated per phospholipid. We expect that saturation of the $(CH_2)_n$ resonance will result in a larger lipid–hydrophobic ion NOE than saturation of the first methylene on the acyl chain, even if the hydrophobic ion is equidistant from the two groups of spins. This is expected because of the larger number of $(CH)_2$ spins per phospholipid. When the important factors in determining the steady-state NOE's are taken into account (distance, number of spins saturated, and segmental order), one can conclude that the hydrophobic ions, when present at low concentrations (<10%), are located in the hydrocarbon region of the bilayer. This is supported by the difference in buildup rates seen for the head group/hydrophobic ion and hydrocarbon/hydrophobic ion NOE's (Figure 5C).

To further localize the hydrophobic ions, we measured time-dependent NOE's when several resonances in the hydrocarbon region were saturated. The time dependence of the NOE buildup is more dependent on distance than is the steady-state NOE because the buildup has a smaller contribution due to spin diffusion. Comparisons of the NOE buildup were previously used to obtain proximity information in phospholipid vesicles (Kuroda et al., 1984; Ellena et al., 1985) and proteins (Dubs et al., 1979; Kumar et al., 1981). The order of hydrocarbon–hydrophobic ion buildup rates is $(CH_2)_n > CH_2CH_2COO > CH_2C{=}C > CH_2COO \approx CH_2CH_3$. Some of the differences between these rates is likely due to the number of spins saturated. In addition, the CH_2CH_2COO peak is only 100 Hz from the $(CH_2)_n$ peak, and saturation of either peak is accompanied by partial saturation of the other. Therefore, the CH_2CH_2COO rate may be anomalously large due to partial saturation of the $(CH_2)_n$ resonance. It is very tempting to ascribe the similarity between the two slowest buildup rates (CH_2COO and CH_2CH_3) to spin diffusion. However, our simulations suggest that spin diffusion should not be dominant. An alternative interpretation is that the hydrophobic ion phenyl groups are at the same depth in the bilayer as the center of the hydrocarbon chains; this is consistent with the observation that the $CH_2C{=}C$ buildup rate is slightly greater than the CH_2CO and CH_2CH_3 rates.

Information provided by previous studies of the binding and kinetics of hydrophobic ions in membranes proves useful in

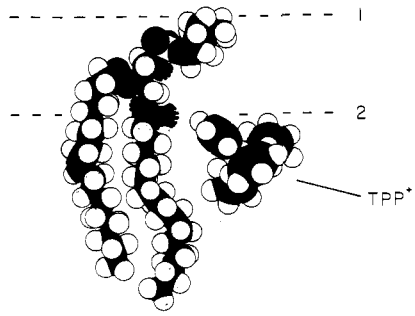

FIGURE 7: Tracing of CPK models showing the average placement of the hydrophobic ion TPP^+ with respect to a phospholipid, POPC, in a bilayer. The placement of this ion is based upon both NOE data and the free energy profiles for hydrophobic ions in membranes (see text).

determining the intramembrane location of hydrophobic ions. Free energy profiles for hydrophobic ions (Figure 1) indicate that the charge center of the ions should lie 3 or 4 Å from groups giving rise to the membrane dipole field (Flewelling & Hubbell, 1986b). These groups have been proposed to be either acyl chain carbonyls or water molecules at the membrane hydrophobic–hydrophilic interface. Capacitance and X-ray diffraction measurements [see Simon and McIntosh (1986)] indicate that water penetrates phospholipid bilayers to the level of the deeper carbonyl group. Taken together, these previous studies and the NOE data presented here are consistent with the placement of the hydrophobic ions depicted in Figure 7. The phospholipid shown in Figure 7 is palmitoyloleoyl-PC (POPC), the dominant species found in egg PC. An average conformation of the phospholipid in the hydrophobic–hydrophilic interface previously established is shown in Figure 7 (Seelig & Seelig, 1980; Hauser et al., 1980, and references cited therein). The hydrophobic ion in this figure is approximately 4 Å from the carbonyl group of the *sn*-1 (palmitoyl) chain. Due to the rather large size of the hydrophobic ion, it can interact with a large portion of the hydrocarbon chain. In addition, due to the chain inequivalence (i.e., the same positions of the *sn*-1 and *sn*-2 chain reside at different depths in the bilayer), the hydrophobic ions interact with somewhat different portions of the two chains. The large size of these ions and the acyl chain inequivalence are likely to account for the similarity of the NOE buildup rates along the alkyl chain.

Membrane bilayers are clearly very dynamic, and Figure 7 is intended to indicate the average position of TPP^+ relative to that of the phospholipid. The exact position of the acyl chains immediately next to the hydrophobic ions will be quite variable, just as it is in bilayers containing no hydrophobic ions (Meraldi & Schlitter, 1981). From Figure 7, one might expect enhanced chain bending around the hydrophobic ion or some interdigitation of lipid from the opposing monolayer to fill the apparent gap resulting from the difference in length between hydrophobic ion and lipid. In fact, the presence of small amounts of TPP^+ in bilayers has been shown to alter phospholipid conformation (Altenbach & Seelig, 1985). However, experiments described above indicate that the alteration is small and that the phospholipid organization is not greatly changed near the hydrophobic ions. For example, the hydrophobic ions have no effect on the ^{13}C spin–lattice and spin–spin relaxation times. In addition, the steady-state NOE's obtained for $TPHP^+$ upon saturation of the phospholipid resonances were very similar to those for TPB^-. If TPB^- enhanced interdigitation, one would expect less interdigitation for $TPHP^+$ (because of its long alkyl chain); hence differences in the NOE's for TPB^- and $TPHP^+$ should be seen. The molecular packing problem suggested in Figure 7 will at least be partially solved by phospholipid conformations that exist prior to the addition of hydrophobic ions. Also, curvature of the membrane surface in the vicinity of the hydrophobic ions may promote efficient packing and have little effect on phospholipid conformation.

Altenbach and Seelig (1985) used ^2H NMR and UV spectroscopy to study the binding of TPP^+ to palmitoyloleoylphosphatidylcholine (POPC). They measured the binding of TPP^+ to POPC over a wide TPP^+ concentration range and observed that TPP^+ altered the quadrupole splitting of head-group deuteriated POPC. This result indicates that TPP^+ has an effect on phospholipid conformation. However, the observed splitting cannot be rigorously interpreted in terms of a specific conformational transition [see Browning (1981) and references therein]. The conformational change may be rather small, which is suggested by their ^{31}P NMR results, and may not necessarily occur in the head group.

There is no significant difference between the relative NOE buildup rates for TPB^- and TPP^+. Thus, the hydrophobic ions appear to have the same general binding location. The energy profile for these ions (see Figure 1) indicates that they occupy locations approximately 1.3 Å apart. One would not expect the NOE buildup rates to be sensitive to such a small distance, and therefore these profiles are consistent with the NOE data.

In summary, we used steady-state, time-dependent, and two-dimensional ^1H NOE spectroscopy to examine the binding location for hydrophobic ions in membranes. At high concentrations, tetraphenylboron associates specifically with the lipid head group of egg PC vesicles. At much lower concentrations, this hydrophobic ion cross-relaxes strongly with protons on the alkyl chains of the phospholipid. For the hydrophobic cation tetraphenylphosphonium, a similar pattern of NOE's is seen at low concentrations. These NOE data are consistent with the free energy profiles for TPP^+ and TPB^-. Taken together, this information provides strong support for the binding location proposed here, which places these ions in the hydrocarbon region of the bilayer.

Registry No. TPP^+, 18198-39-5; TPB^-, 4358-26-3.

REFERENCES

Altenbach, C., & Seelig, J. (1985) *Biochim. Biophys. Acta 818*, 410–415.

Andersen, O. S., Feldberg, H., Nakadomari, H., Levy, S., & McLaughlin, S. (1978) *Biophys. J. 21*, 35–70.

Brown, M. F. (1982) *J. Chem. Phys. 77*, 1576–1599.

Browning, M. F. (1981) *Biochemistry 20*, 7123–7133.

Burnell, E. E., Cullis, P. R., & DeKruijff, B. (1980) *Biochim. Biophys. Acta 603*, 63–69.

Cafiso, D. S., & Hubbell, W. L. (1981) *Annu. Rev. Biophys. Bioeng. 10*, 217–244.

Cafiso, D. S., & Hubbell, W. L. (1982) *Biophys. J. 39*, 263–272.

Clore, G. M., & Gronenborn, A. M. (1983) *J. Magn. Reson. 53*, 423–442.

Craik, D. J., & Levy, G. C. (1984) *Top. Carbon-13 NMR Spectrosc. 4*, 239–275.

Dobson, C. M., Olejniczak, E. T., Poulsen, F. M., & Ratcliffe, R. G. (1982) *J. Magn. Reson. 48*, 97–110.

Dubs, A., Wagner, G., & Wüthrich, K. (1979) *Biochim. Biophys. Acta 577*, 177–194.

Ellena, J. F., Hutton, W. C., & Cafiso, D. S. (1985) *J. Am. Chem. Soc. 107*, 1530–1537.

Flewelling, R. F., & Hubbell, W. L. (1986a) *Biophys. J. 49*, 531–540.
Flewelling, R. F., & Hubbell, W. L. (1986b) *Biophys. J. 49*, 541–552.
Hauser, H., Guyer, W., Pascher, I., Skrabal, P., & Sundell, S. (1980) *Biochemistry 19*, 366–373.
Hubbell, W. L., Cafiso, D. S., & Brown, M. F. (1980) *Fed. Proc., Fed. Am. Soc. Exp. Biol. 39*, 1983.
Ketterer, B., Neumcke, B., & Läuger, P. (1971) *J. Membr. Biol. 5*, 225–245.
Kumar, A., Wagner, G., Ernst, R., & Wüthrich, K. (1981) *J. Am. Chem. Soc. 103*, 3654–3658.
Kuroda, Y., & Kitamura, K. (1984) *J. Am. Chem. Soc. 106*, 1–6.
Läuger, P., Benz, R., Stark, G., Bamberg, E., Jordan, P. C., Fahr, A., & Brock, W. (1981) *Q. Rev. Biophys. 14*, 513–598.
LeBlanc, O. H. (1969) *Biochim. Biophys. Acta 193*, 350–360.
Levine, B. A., Sackett, J., & Williams, R. J. P. (1979) *Biochim. Biophys. Acta 550*, 201–211.
McLaughlin, S. (1977) *Curr. Top. Membr. Transp. 9*, 71–144.
Meraldi, J. P., & Schlitter, J. (1981) *Biochim. Biophys. Acta 645*, 193–210.
Morris, G. A. (1986) *Magn. Reson. Chem. 24*, 371–403.
Mulders, F., van Langen, H., van Ginkel, G., & Levine, Y. K. (1986) *Biochim. Biophys. Acta 859*, 209–218.
Neumcke, B., & Läuger, P. (1970) *J. Membr. Biol. 3*, 54–66.
Noggle, J. H., & Schirmer, R. E. (1971) *The Nuclear Overhauser Effect*, Academic, New York.
Pace, R. J., & Chan, S. I. (1982) *J. Chem. Phys. 76*, 4241–4247.
Pickar, A. D., & Benz, R. (1978) *J. Membr. Biol. 44*, 353–376.
Seelig, J., & Seelig, A. (1980) *Q. Rev. Biophys. 13*, 19–61.
Seidah, N. G., Roy, G., Laprade, R., Cyr, T., & Dugas, H. (1976) *Can. J. Biochem. 54*, 327–335.
Siminovitch, D. J., Brown, M. F., & Jeffrey, K. R. (1984) *Biochemistry 23*, 2412–2420.
Simon, S. A., & McIntosh, T. J. (1986) *Methods Enzymol. 127*, 511–521.
Singleton, W. S., Gray, M. S., Brown, M. L., & White, J. L. (1965) *J. Am. Oil Chem. Soc. 42*, 53–57.
States, D. J., Haberkorn, R. A., & Ruben, D. J. (1982) *J. Magn. Reson. 48*, 286–292.
Wagner, G., & Wüthrich, K. (1979) *J. Magn. Reson. 33*, 675–680.

Role of C-Terminal Tail of Long Neurotoxins from Snake Venoms in Molecular Conformation and Acetylcholine Receptor Binding: Proton Nuclear Magnetic Resonance and Competition Binding Studies

Toshiya Endo* and Masanao Oya
Department of Chemistry, College of Technology, Gunma University, Kiryu 376, Japan
Nobuo Tamiya
Department of Chemistry, Faculty of Science, Tohoku University, Aobayama, Sendai 980, Japan
Kyozo Hayashi
Department of Biology, Gifu Pharmaceutical University, Mitahora, Gifu 502, Japan
Received October 8, 1986; Revised Manuscript Received February 24, 1987

ABSTRACT: The role of the "C-terminal tail" segment of long neurotoxins has been investigated. The C-terminal four to five residues of α-bungarotoxin and Laticauda colubrina b have been cleaved off by carboxypeptidase P. The effect of such deletion on the toxin conformation has been monitored in proton nuclear magnetic resonance spectra and circular dichroism spectra. The removal of the C-terminal residues primarily affects the chemical shifts of proton resonances of the residues close to the cleavage site and does not induce a major conformational change. Therefore, the C-terminal tail of long neurotoxins does not appear to be important in maintaining the specific polypeptide chain folding. On the other hand, competition binding with tritium-labeled toxin α to *Narke japonica* acetylcholine receptor has revealed that cleavage of the C-terminal residues reduces the binding activity of α-bungarotoxin or Laticauda colubrina b to acetylcholine receptor. Thus it is likely that (the basic amino acid residues in) the C-terminal tail is directly involved in the binding of long neurotoxins to electric organ (and muscle) acetylcholine receptor.

Venoms of proteroglyphous snakes (cobras and sea snakes) contain small curaremimetic proteins called neurotoxins [reviewed by Dufton and Hider (1983)]. The neurotoxin binds specifically to the nicotinic acetylcholine receptor (AChR)[1] in the postsynaptic membranes of vertebrate muscle and fish electric organs, prevents the binding of chemical neurotransmitter acetylcholine, and thereby blocks the nerve impulses. At present, amino acid sequences of about 80 neurotoxins are available, and they form a large family of homologous proteins, which can be further divided into two subgroups, namely, short neurotoxins and long neurotoxins. Long neurotoxins have an

* Address correspondence to this author at Biocenter, University of Basel, CH-4056 Basel, Switzerland.

[1] Abbreviations: AChR, nicotinic acetylcholine receptor; α-Bgt, α-bungarotoxin from *Bungarus multicinctus*; Lc b, Laticauda colubrina b from *Laticauda colubrina*; Tx α, toxin α from *Naja nigricollis*; CPase, carboxypeptidase; NMR, nuclear magnetic resonance; CD, circular dichroism; Tris-HCl, tris(hydroxymethyl)aminomethane hydrochloride; EDTA, ethylenediaminetetraacetic acid; EGTA, ethylene glycol bis(β-aminoethyl ether)-*N,N,N',N'*-tetraacetic acid.

0006-2960/87/0426-4592$01.50/0